Journal of Nuclear Materials 265 (1999) 22–27

journal of nuclear materials

Angular dependence of the sputtering yield of rough beryllium surfaces

M. Küstner [a], W. Eckstein [a,*], E. Hechtl [b], J. Roth [a]

[a] *Max-Planck-Institut für Plasmaphysik, EURATOM-Association, Boltzmannstr.2, D-85748 Garching, bei Munchen, Germany*

[b] *Technische Universität, Lichtenbergstr.4, D-85747 Garching, bei Munchen, Germany*

Received 1 July 1998; accepted 8 October 1998

Abstract

A new approach to study the influence of target surface roughness on sputtering is applied for two differently prepared beryllium surfaces. The topography of the Be surfaces are monitored with a scanning tunnelling microscope (STM). Mathematical methods are used to determine a distribution of local angles of incidence for a given nominal angle of incidence; this distribution is taken as input for the Monte Carlo program TRIM.SP for the calculation of the sputter yield of rough surfaces. Additionally, the redeposited fraction of emitted atoms on the rough surface is taken into account. The calculated results are compared with the calculation for an atomically smooth surface and experimental sputter yields. Results are given for deuterium and helium, and selfbombardment at 0.3 and 3 keV and several angles of incidence for rough Be surfaces.

1. Introduction

Be is a candidate for a plasma facing material in ITER [1,2]. Therefore, it is important to know its behaviour under hydrogen or deuterium ion bombardment, in particular, its erosion behaviour [3–5]. The physical sputter yield depends on the target material, the projectile species and their energy and incidence angle. For the angular dependence of the sputter yield an empirical formula is given by Yamamura et al. [6]:

$$\frac{Y(E_0,\alpha)}{Y(E_0,0)} = \frac{e^{(f[1-\frac{1}{\cos\alpha}]\cos\alpha_{opt})}}{\cos^f\alpha}, \quad (1)$$

where $Y(E_0,\alpha)$ is the yield at ion energy E_0 and nominal angle of incidence α. The quantities f and α_{opt} are parameters to fit the data; α_{opt} is the nominal incidence angle at maximum yield. Generally, the yield increases from perpendicular incidence to a maximum at $\alpha = 55°$ to 85°, and then decreases due to the strong reflection at grazing incidence.

This is the situation for atomically smooth surfaces for which the TRIM.SP Monte-Carlo program [7,8] is widely used and produces good results [9]. Measured sputter yields for rough surfaces differ as much as a factor of five from measured yields for well polished surfaces near the maximum [10–12]. The general observation is that for rough surfaces compared to smooth surfaces the yield is larger at perpendicular incidence and smaller in the region of the maximum.

An approach favoured by Ruzic et al. [13–16] used results of adsorption measurements [17–19] which showed that the roughness of some surfaces can be described by a fractal dimension. This model is in good agreement with reflection experiments [20] but disagrees with the sputtering data. One disadvantage is that not all rough surfaces may be described by a fractal structure. To overcome this restriction we have proposed a different approach [21].

In the first step the surface topography is measured with an STM. With this method one gets the height information at points in equal distances [22–25]. The second step is to construct the surface with these pixel files. Then the surfaces have to be analysed for the distribution of the local angles of ion incidence and for the fraction of emitted atoms, which is redeposited on the

* Corresponding author. Tel.: +49-89 3299 1259; fax: +49-89 3299 1149; e-mail: wge@ipp.mpg.de

PII: S0022-3115(98)00648-5

rough surface. This distribution of local incidence angles replaces the fixed nominal angle of incidence as input for the Monte-Carlo program TRIM.SP which is then applied to calculate the yield for a rough surface. The redeposition fraction is a global factor for each surface.

2. Sputtering experiment

In this sputtering experiment the irradiations were performed with a Harwell-type isotope separator [26]. Beryllium fluoride was used as charge material in the ion source. The sputtering yield was determined by the weight change method. The loss or gain of target material due to the ion irradiation was measured by an ultramicrobalance (Sartorius S4). Its accuracy is 1 μg. To adjust ion incidence angle and energy an ion optical decelaration system [27] was used to retard the high-energy ion beam from the isotope separator in front of the sputtering sample. The Be^+ fluence was determined by current integration with an accuracy of 1%. Actually the sputtering yield Y_{ex} by this method is the sum of the sputtering yield and the particle reflection coefficient R_N [28]:

$$Y_{ex} = Y + R_N = 1 - \frac{\Delta m N_0}{N_1 M_2}, \tag{2}$$

where Δm is the target mass change, N_1 is the number of projectiles, M_2 the atomic mass of the target atoms, N_0 is Avogadro's number. Additionally, previously published data for D and He sputtering [3,4] are analysed using the roughness model.

3. Topographic measurements

To analyse the surface topography by the distribution of local angles of incidence and the redeposition fraction one needs a representative area of the surface with maximum resolution [29,21]. The representative part of a surface is defined here as the smallest area in which the distribution of local angles of incidence does not depend on the position of investigation.

For analysing the measurement the pixel files are used to construct the surface with elementary triangular planes. The size of these triangles depends on the distance of the points at which the height of the surface is measured. The triangles should be big enough to neglect edge effects. As a criterion we define that more than 99% of target atoms sputtered by incidence ions on the triangle should leave the target from the same triangle [29,21]. This is the condition for the minimum size for the elementary triangle of the constructed surface. Smaller triangles do not allow to calculate redeposition because a significant number of the sputtered atoms cannot be allocated to the triangle hit by the incident ions.

It is important to select the point distance of the height measurement due to the resolution of the STM measurement, because the most important surface structures which dominate the distribution of local angles of ion incidence are the small ones. This can be shown by analysing the surface measurements with the methods of wavelet transforms and height correlation function [29,21].

Once the size of the representative area of the surface and the reasonable resolution are known, the surface topography of Be can be measured by the STM method. We used a commercial device (Rasterscope/3000, Danish Micro Engineering A/S) and measured the surfaces in air for a fast and easy sample change.

In Figs. 1 and 2 the surfaces of two different Be samples are shown. Fig. 1(a) depicts a highly polished Be surface before sputtering. The representative target surface with a size of 7.9×7.9 μm^2 is very smooth and the maximum difference of altitude amounts to 0.5 μm. After sputtering the surface with 3.0 keV Be ions the surface roughened and reached a dynamic equilibrium of sputtering which means same yields in equal time steps at a constant ion flux. The surface which can be seen in Fig. 1(b) has the same size as before but the maximum difference of altitudes now amounts to 1.2 μm.

4. Model

Surface roughness influences the sputtering yield by two effects, the angular distribution of local ion incidence and the redeposition fraction. These two effects will be described. A detailed description and analysis of the measured pixel files is given in Refs. [29,21].

On a rough surface incident ions do not have the same angle of incidence at any location. Taking a measured surface and construct it by elementary triangles from the pixel file one can calculate all local angles of incidence σ_{ij} between the normal vectors of the triangles and the ion beam. These local angles of incidence depend on the nominal angle of incidence, α, of the ion beam. Filling them into a histogram and normalising it one gets the distribution of local angles of incidence $\rho(\sigma_{ij}(\alpha), \alpha) = \rho(\alpha)$.

For higher incidence angles the yield increases. Replacing the fixed nominal angle, α, by the distribution $\rho(\alpha)$ in the simulation code TRIM.SP must give a higher yield at $\alpha = 0°$ for rough surfaces. The yield should be the higher the rougher the surface is, because the normalized distribution will broaden. At high nominal angles the distribution, $\rho(\alpha)$, contains contributions from smaller local angles of ion incidence. As a result the maximum yield for a rough surface should be smaller than the one for a smooth surface.

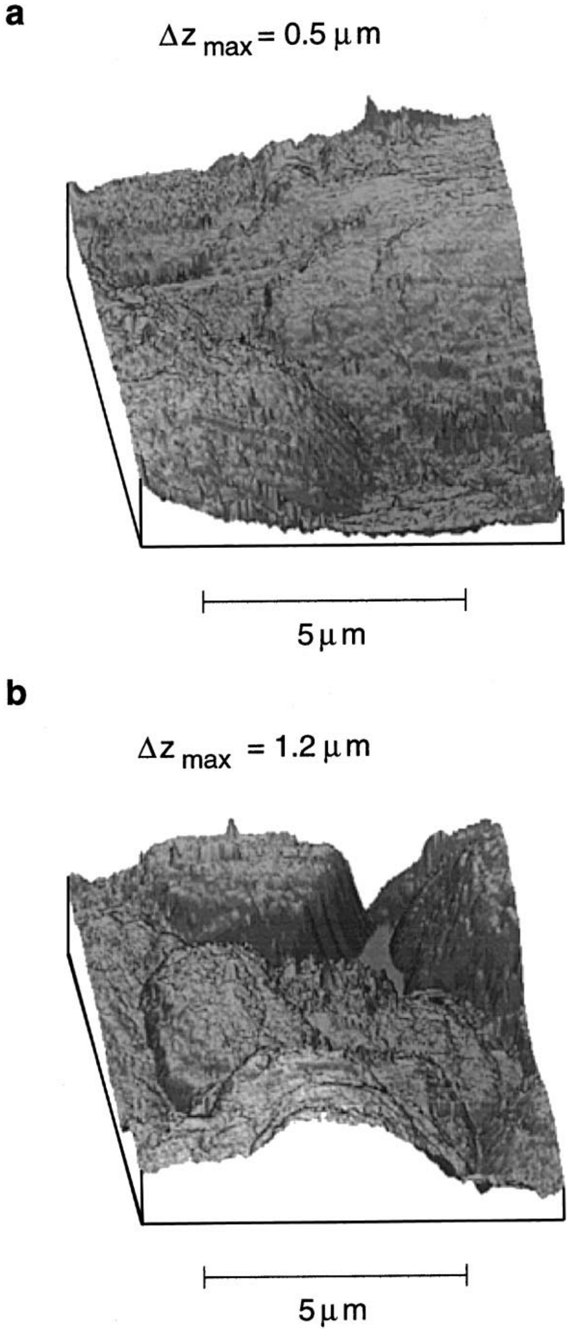

Fig. 1. The topography of polished Be has been measured with an STM in air. The surface has been monitored before sputtering (a) and after sputtering to the dynamic sputtering equilibrium (b). Ion bombardment roughened the Be surface to a very coarse topography. The picture size amounts to 7.9×7.9 µm^2 and the maximum height difference amounts to 0.5 µm for the polished Be surface (a) and 1.2 µm for the roughened Be surface (b).

Until this point the redeposition of sputtered target atoms as the second effect is not yet taken into account. It is assumed that the sputtered atoms leave the elementary triangles in form of a spherical cosine distribution. The trajectory of the sputtered target atoms is followed until they finally leave the surface or they hit it again. At the location where the atoms hit the target surface again they are assumed to be deposited with no further processes such as collisions, secondary sputtering, reflection or transmission. The number of sputtered target atoms per incident ion depends to the local angle of incidence. The triangles constructing the surface are assumed to be smooth on an atomic scale, and the local yield is calculated with the Yamamura formula, Eq. (1). It is assumed that all sputtered atoms leave the surface at the centre of the triangles. Geometric conditions of the surface lead to a cut-off of segments of the cosine sphere as shown in Fig. 3. The volume of this part of the sphere which is shadowed by the geometry divided by the whole sphere is the redeposition fraction $R'_{ij}(\sigma_{ij}(\alpha), \alpha)$ for the elementary triangle. The sum over all elementary triangles normalized with the size of the measured surface F gives the redeposition fraction for the surface:

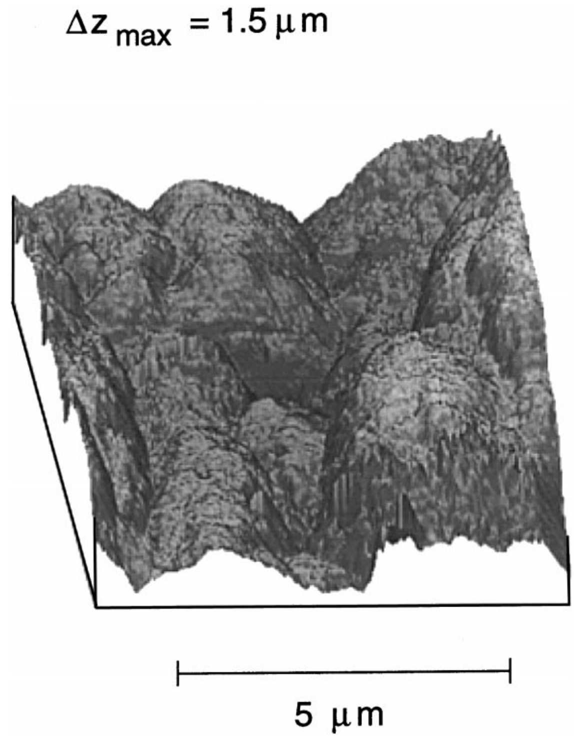

Fig. 2. The picture shows a rough Be surface. It is not polished and does not change its typical structure under ion bombardment. The size amounts to 7.9×7.9 µm^2 with a maximum height difference of 1.5 µm. This Be target is manufactured in a different way to the target in Fig. 1.

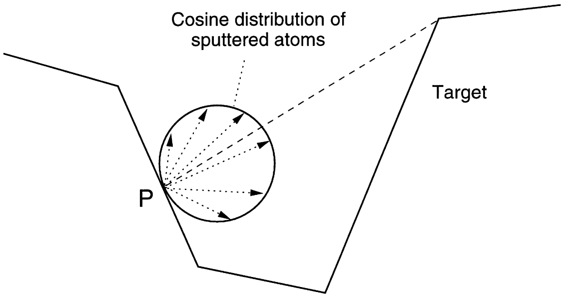

Fig. 3. Target atoms sputtered by an incident ion are leaving the surface at a point P cosine distributed. The size of the cosine sphere depends on σ. Some of the sputtered atoms are redeposited on the surface. The line between P and the edge cuts off a segment from the cosine sphere. The volume of these segment divided by the volume of the sphere gives the redeposition fraction $R(\sigma)$.

$$R(\alpha) = \frac{1}{F}\sum_{ij} R'_{ij}(\sigma_{ij}(\alpha), \alpha). \tag{3}$$

This effect reduces the yield generally and will be more important the rougher the surface is. $R(\alpha)$ is a number between 0 and 1. $Y'(\alpha)$ calculated with the modified TRIM.SP has to be corrected with the redeposition fraction:

$$Y_{\text{th}}(\alpha) = Y'(\alpha)(1 - R(\alpha)). \tag{4}$$

The model assumes a static surface; the surface topography structure is not modified by ion bombardment.

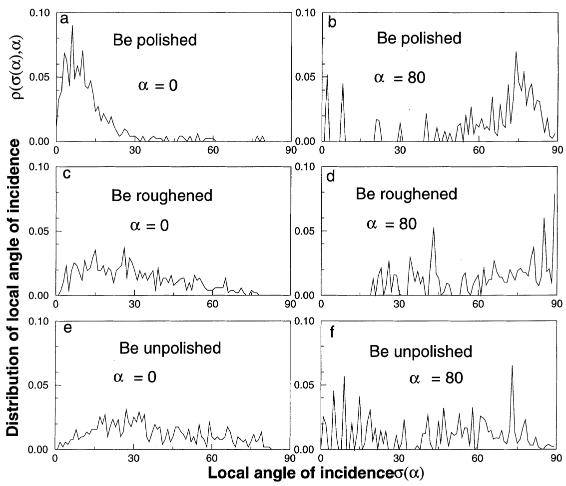

Fig. 4. Distributions of the local angles of incidence $\rho(\sigma(\alpha), \alpha)$ are plotted versus the local angle σ. The distributions are extracted from the surfaces in Fig. 1 and Fig. 2. For every surface the distributions of local angles of ion incidence are shown for the two nominal angles $\alpha = 0°$ and $\alpha = 80°$. In (a) and (b) the distributions for polished Be are shown, in (c) and (d) for roughened Be by ion bombardment, and in (e) and (f) for the rough Be.

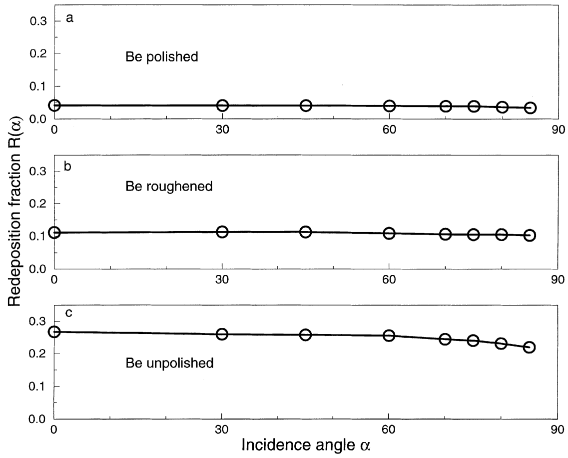

Fig. 5. The redeposition fraction $R(\alpha)$ is plotted versus the nominal angle of ion incidence, α. Fig. 5(a) shows $R(\alpha)$ for the polished Be surface and (b) for the roughened Be surface. The redeposition fraction is negligible for a smooth surface but has to be taken into account for a roughened surface. In Fig. 5(c) $R(\alpha)$ is plotted for the rough surface and it can be seen that the redeposition is important for rough surfaces.

Thus, the method is restricted to surfaces in their dynamic sputtering equilibrium which means equal yields in same time steps by constant ion flux.

5. Results and discussion

The Be surface topographies in Figs. 1 and 2 are STM pictures of a polished Be surface (Fig. 1(a)) and of

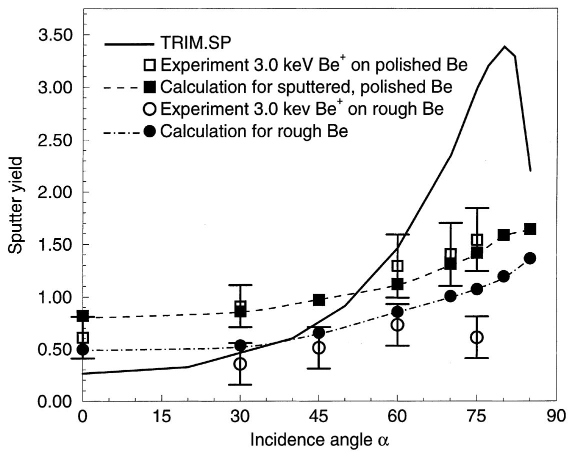

Fig. 6. The sputter yield is plotted versus the nominal angle of ion incidence, α. The calculation for the polished (filled squares) and the rough Be surface (filled circles) is compared with the experimental data for these targets (open squares and circles) and the simulation for an atomically smooth Be surface (solid line).

a polished Be target but roughened by ion bombardment (Fig. 1(b)), whereas in (Fig. 2) the surface topography of a unpolished surface is shown. The surface topography in Fig. 1(b) is measured in the dynamic sputtering equilibrium with 3.0 keV Be^+ ions where the sputter yield does not change with further bombardment. The representative size of the pictures has been determined to 7.9×7.9 μm^2 with 256^2 pixels each. The maximum height difference amounts to 1.5 μm for the rough Be surface and to 0.5 μm for the polished surface. After bombarding the surface with 3.0 keV Be^+ ions the surface is roughened and the maximum height difference is 1.2 μm. The unpolished surface is very similar to the surface roughened by the ion beam.

These measurements of surface topography have to be analysed for the distribution of local angles of ion incidence and the redeposition fraction. In Fig. 4 the distributions for the three surfaces at the nominal ion incidence angle of $\alpha = 0°$ and $\alpha = 80°$ are shown. A polished Be target with its smooth surface, see Fig. 1(a), has a distribution of local angles of incidence distribution which peaks sharply around the nominal angle of incidence (Fig. 4(a) and (b)). Its centre is at 13° for perpendicular ion incidence and 63° for $\alpha = 80°$. The unpolished Be surface (Fig. 4(e) and (f)) and the Be surface roughened by ion bombardment (Fig. 4(c) and (d)) show broad distributions and the centres of the distributions are shifted to higher angles for $\alpha = 0°$ (roughened: 30°; unpolished: 38°) and to smaller angles for $\alpha = 80°$ (roughened: 49°; unpolished: 44°). The distributions for the two surfaces look as similar as the corresponding topographies but there are significant differences in their higher moments.

The redeposition fraction $R(\alpha)$ for the three surfaces is shown in Fig. 5 for different nominal angles of ion incidence. It can be seen that the redeposition fraction

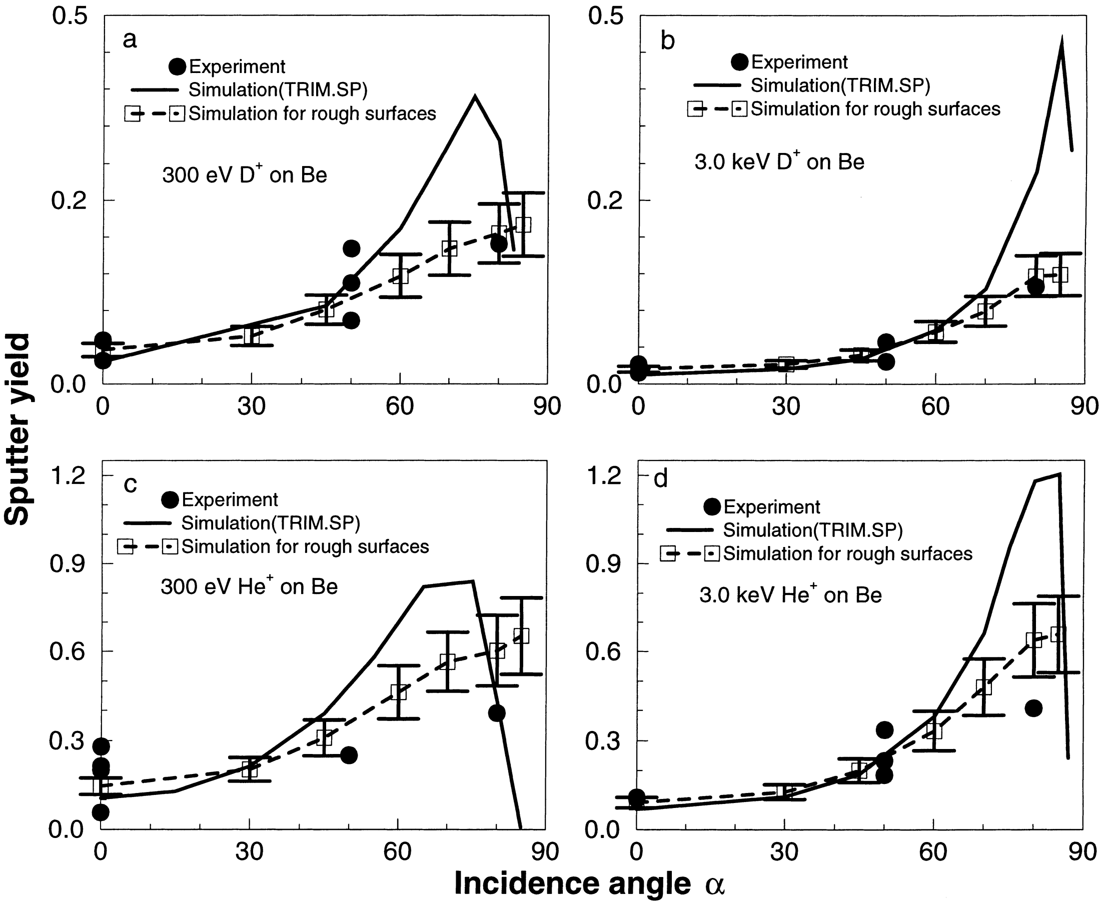

Fig. 7. In Fig. 7(a)–(d) the sputter yield is plotted versus the nominal angle of ion incidence, α. In (a) and (b) the experimental data and calculations for bombardment with D^+ at 300 eV (a) and 3.0 keV (b) are shown. (c) and (d) show the results for bombardment with He^+ of the same energies. The filled circles represent the experimental data and the smooth lines show the results for atomically smooth surfaces. The open squares represent the results for the calculations for rough Be surfaces. They are connected with a dashed line to guide the eye.

for a polished Be surface is negligible (Fig. 5(a)) but it is an important correction for the unpolished surfaces. About 25% of the sputtered target atoms of the rough Be surface are redeposited (Fig. 5(c)), only at glancing ion incidence the redeposition decreases because only the ridges of the topographic structures are hit by the ion beam where the redeposition is low. The redeposition is also important for the roughened Be surface (Fig. 5(b)). It amounts to 10%, and the decrease at glancing angle of ion incidence is less pronounced. With Eq. (3) we get the theoretical yield $Y_{\mathrm{th}}(\alpha)$ as the product of $Y'(\alpha)$ and $1 - R(\alpha)$. The results for the roughened and the unpolished Be surfaces are plotted in Fig. 6. These results are compared with the TRIM data for an atomically smooth surface (solid line), the sputtering data for the Be surface in a dynamic sputtering equilibrium and the sputtering data for the unpolished surface. The experimental data are in good agreement with the calculations for the unpolished and the roughened surface. On the other hand the calculation for an atomically smooth surface disagrees with the experimental data. The significant difference between the roughened and the unpolished surface in calculation and experiment seems to be mainly due to a larger redeposited fraction for the unpolished surface. The origin of this difference may be due to different manufacturing.

To validate the model the calculated yields of a roughened Be surface for the projectiles He^+ and D^+ with the energies 0.3 and 3.0 keV are compared with the sputtering data and the calculations for atomically smooth surfaces. Fig. 7 shows the results. In every case the calculation for the unpolished Be surface is in much better agreement with the sputtering data than TRIM.SP calculations for smooth surfaces.

6. Conclusions

A new method to analyse the influence of surface roughness on the angular dependence of the sputter yield is applied to the sputtering of rough Be targets. In a first step the representative size of the surface has to be determined. The surface topography is monitored with an STM in air which allows a very simple and fast change of the sample.

The distribution of the local angles of ion incidence is determined and used as input to the Monte-Carlo program TRIM.SP to calculate the sputter yield for the rough surface. This result is corrected with the redeposition fraction. The yields calculated along these lines are compared with measured sputter yields for D^+, He^+, and Be^+ bombardment at several angles of incidence.

While TRIM.SP calculations for smooth surfaces in all cases show an pronounced increase with angle of incidence, the implementation of the distribution of local angles of incidence into the code leads to a much better agreement with experimental data. The redeposition is more important for originally unpolished surfaces and must be taken into account for best agreement.

References

[1] M.F. Smith, W. Mullendore, J. Nucl. Mater. 122 (1984) 855.
[2] K.L. Wilson, R.A. Causey, W.L. Hsu, B.E. Mills, M.F. Smith, J.B. Whitley, J. Vac. Sci. Technol. A 8 (1990) 1750.
[3] J. Bohdansky, J. Roth, J. Nucl. Mater. 123 (1984) 1417.
[4] J. Roth, W. Eckstein, J. Bohdansky, J. Nucl. Mater. 165 (1989) 199.
[5] C.H. Wu, E. Hechtl, H.R. Yang, W. Eckstein, J. Nucl. Mater. 176/177 (1990) 845.
[6] Y. Yamamura, Y. Itikawa, N. Itoh, Nagoya University Institute of Plasma Physics Report IPPJ-AM-26, 1983.
[7] W. Eckstein, Computer Simulation of Ion-Solid Interaction, Springer Series in Material Science, vol. 10. Springer, Berlin, 1991.
[8] J. Biersack, W. Eckstein, Appl. Phys. A 34 (1984) 73.
[9] W. Eckstein, J. Bohdansky, K. Kamada, J. Nucl. Mater. 150 (1987) 266.
[10] J. Roth, W. Eckstein, E. Gauthier, J. László, J. Nucl. Mater. 179/181 (1991) 34.
[11] E. Gauthier, W. Eckstein, J. László, J. Roth, J. Nucl. Mater. 176/177 (1989) 438.
[12] Y.N. Zhukova, E.S. Mashkova, V.A. Molchanov, V.M. Sotnikov, W. Eckstein, Povernost Fysika, Chemiya, Mechanica 89 (1994) 107.
[13] A. Myers, J. Doyle, D. Ruzic, J. Appl. Phys. 72 (1992) 3064.
[14] D. Ruzic, In: S. Rossnagel, J. Cuomo, W. Westwood (Eds.), Handbook of Plasma Processing Technology, Noyes Publications, 1989.
[15] D. Ruzic, Nucl. Instr. Meth. B 47 (1990) 118.
[16] M. Shaheen, D. Ruzic, J. Vac. Sci. Technol. A 11 (1993) 3085.
[17] D. Avnir, D. Farin, P. Pfeifer, J. Chem. Phys. 79 (1983) 3566.
[18] D. Avnir, D. Farin, P. Pfeifer, Nature 308 (1984) 261.
[19] I. Ismail, P. Pfeifer, Langmuir 10 (1994) 1532.
[20] M. Mayer, W. Eckstein, B.M.U. Scherzer, J. Appl. Phys. 77 (1995) 6609.
[21] M. Küstner, W. Eckstein, V. Dose, J. Roth, Nucl. Inst. Meth. B, 145 (1998) 320.
[22] J. Tersoff, D. Hamann, Phys. Rev. B 31 (1985) 805.
[23] P. Hansma, V. Elings, O. Marti, C. Bracker, Science 242 (1988) 209.
[24] N. Almquist, Surf. Sci. (1996).
[25] E. Eklund, R. Bruinsma, J. Rudnick, R. Williams, Phys. Rev. Lett. 76 (1991) 1759.
[26] E. Hechtl, Nucl. Instr. Meth. B 26 (1987) 37.
[27] E. Hechtl, Nucl. Instr. Meth. B 70 (1992) 441.
[28] E. Hechtl, W. Eckstein, J. Roth, Nucl. Instr. Meth. B 90 (1994) 505.
[29] M. Küstner, dissertation, Universität Bayreuth, 1997.